OPTOELECTRONICS AND ADVANCED MATERIALS – RAPID COMMUNICATIONS Vol. 1, No. 2, February 2007, p. 77 - 85

An overview on the solid byproducts of the galvanizing kettle

G. VOURLIAS, N. PISTOFIDIS, G. STERGIOUDIS, E. K. POLYCHRONIADIS*
Department of Physics, Aristotle University of Thessaloniki, GR 54124 Thessaloniki, Greece

In galvanizing process several byproducts are formed. Among them solid materials composed of different compounds are grown in the galvanizing kettle. The present work examines the structure of the galvanizing ashes, bottom dross and blowing waste with Scanning Electron Microscopy (SEM), Transmission Electron Microscopy (TEM) and X-Ray Diffraction (XRD). From this research it was deduced that these byproducts are mainly composed of different zinc compounds, while a large amount of iron in the form of oxides or Fe-Zn intermetallics is also present. In any case, the examined materials are suitable for zinc recovery, although their composition and the structure is highly different in every case.

(Received December 2, 2006; accepted January 12, 2007)

Keywords: Metals and alloys, Coating materials, X-ray diffraction, SEM, TEM

1. Introduction

Hot dip galvanizing is one of the most effective corrosion protection methods for steel and iron substrates [1]. However, although the anticorrosive performance of the hot dip galvanized products is very high and as a result this method is very advantageous, the production of galvanized objects involves the generation of several byproducts. Among them, the galvanizing dross, which amounts to 5-7% of the zinc consumed by the coating formation [2], is one of the most important.

Galvanizing dross is formed inside or on top of the molten zinc [1]. Therefore, it can be classified as floating or bottom dross. The floating dross (also known as "galvanizing ashes") consists mainly of zinc and/or aluminum oxides and chlorides [1], while the bottom dross consists exclusively by intermetallic compounds, such as Al-saturated δ ($FeZn_7$) phase [1]. Intermetallic compounds were also identified in the floating byproduct, but in this case the main component which was reported is $Fe_2Al_5Zn_x$ [1]. Both floating and bottom dross contain also a large amount of solidified zinc, which is traped in liquid form in the device used for their removal from the zinc bath.

The intermetallics of the floating and bottom dross are formed when the concentration of Al and Fe in the zinc kettle is above their solubility limits at a certain temperature. As a result their formation is unavoidable even in the case of perfect management of the zinc bath, because the deliberate Al additions, the Fe dissolution from the immersed objects and the kettle walls as well as the temperature uniformity are very difficult to be controlled [1]. This phenomenon is also enhanced by the Ni addition [3-4], which is used as a medium to inhibit the Sandelin effect (the formation of Fe-Zn alloys up to the surface of the galvanized coating [5]). Also, the formation of the surface oxides, which are present in the ashes, is also impossible to be inhibited, since both Zn and Al are reactive metals and at the temperature of the zinc bath (about 450 ^oC [1]) their reactivity is extremely high. Consequently their reaction with the atmospheric oxygen is inevitable.

The presence of ashes and bottom dross in the molten zinc is undesirable because, as their particles float or suspend inside the liquid metal, they could be trapped inside the coating and cause a common fault known as "coating pimples" [6], resulting to a low quality coating. Therefore it is necessary to be regulary removed from the kettle. Especially the oxides formed on top of the bath are removed every time an object is immersed in the molten zinc.

Another byproduct, formed only at the tube galvanizing facilities during the finishing of the galvanized coating, is the blowing waste. After a tube emerges from the galvanizing bath, its inner surface is subjected to a compressed air wiping, in order to diminish its roughness and consequently lower the flow resistance. This way, a very thin powder is produced, which is mainly composed by Zn and ZnO [7].

However, these by-products are not useless. By contrast, Zn is possible to be recovered from them thanks to its high concentration [2, 7-8]. Consequently, they are a valuable row material. Therefore it is very important to be fully characterized, so as to collect data useful for their recycling. Furthermore their characterization could lead to a better understanding of the galvanizing process, resulting to its optimization and the minimization of their production. The above-mentioned researches [2, 7-8] focus only on Zn recovery process. Apart from a brief characterization consisting of a rough chemical analysis of each byproduct, nothing else is reported. On the other hand, other studies [1 and references herein], that examine hot-dip galvanizing thoroughly, offer very little information on the compounds that compose floating and bottom drosses, without going into details. Furthermore this information refers only to the continuous galvanizing lines, while the blowing waste is not even reported.

More detailed research papers were recently published [9-10] where the floating dross [9], the bottom dross [10] and the blowing waste [10] were examined. As far as it concerns floating dross [9] an effort was made to correlate its presence with the outburst formation in continuous galvanizing lines. From this research it was elucidated that floating dross contains a complex oxide of the $ZnAl_{2-x}Fe_yO_4$ stoichiometry that belongs to the spinel solid solution series and seems to be the mot problematic. This oxide accelerates the breakdown of the Fe-Al passive layer because it facilitates Zn diffusion through the interface oxide/Fe_2Al_5 layer and it results to the formation of a series of Fe-Zn intermetallic phases by an outburst growth. The Fe-Zn phases could precipitate on the coating surface leading to a degradation of its quality. On the other hand bottom dross [10] is insoluble and more dense than liquid zinc. As a result it precipitates on the kettle floor. Therefore the final byproduct after its removal from the liquid metal contains large amounts of Zn. However bottom dross does not seem to interact with the growth mechanism of the coating, apart from the fact that its crystals could precipitate on the coating reducing its appearence. Finaly the blowing waste [10] is formed outside the kettle. Consequently it has no effect on the coating growth. However it is very reach in zinc since it is formed from the eta phase which is composed by pure Zn. Furthermore it is powdery, which could be a grate advantage for the zinc smelting industry.

In the present work the research on this topic is summarized and focused on batch hot-dip galvanizing lines. As a result a detailed reference is presented dealing with all the possible undesirable solid materials forming in the zinc kettle. Blowing waste is also enclosed because it could be used in a similar way with floating and bottom dross. However the gaseous byproducts and the semi-solid materials (sludges) formed in previous stages of the galvanizing process are not examined. This work intends to present with completeness the examination of the structure, the morphology and the chemical composition of the galvanizing byproducts, without including the recycling methods. Hence it could be used as the main reference for researchers dealing with the waste treatment problem.

2. Experimental

A rough flow sheet of a typical hot-dip galvanizing line is presented in Fig. 1. Both floating and the bottom dross samples were provided batch hot-dip galvanizing facilities. These samples were collected right after being removed from the zinc kettle, while the blowing waste was provided by a tube mill. The samples of the clean zinc bath and the pure zinc ingots were provided by the same industries. The zinc bath was considered "clean" right after the usual removal of the bottom and floating dross, as it is performed in the industry (mechanicaly with the usage of suitable shovels). The samples of the clean bath were collected with a special device from three different depths (10, 100 and 150 cm bellow the zinc surface).

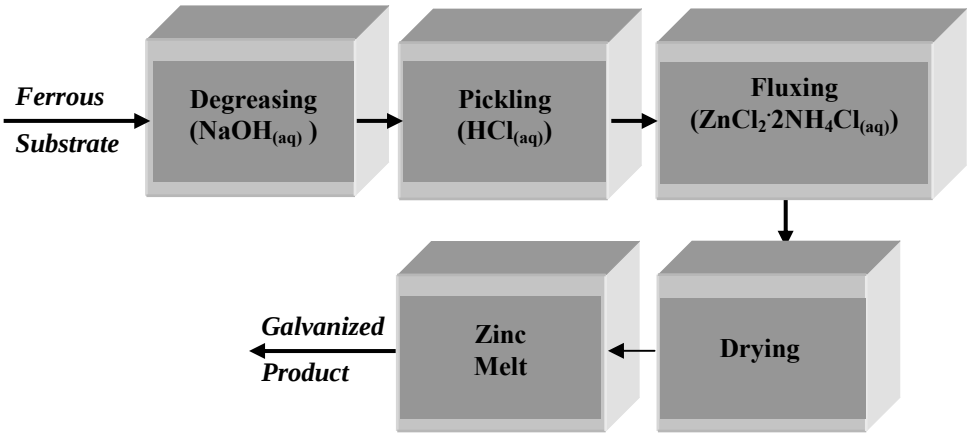

Fig. 1. Schematic diagram of a typical batch hot-dip galvanizing line. The chemical substances used in every step are presented in the brackets. The index (aq) implies aqueous solution.

The examination of the samples took place with X-Ray Diffraction (XRD), Scanning Electron Microscopy (SEM) and Conventional Transmission Electron Microscopy (CTEM). For the examination with XRD a two-cycles SEIFERT 3003 TT diffractometer was used with FeKα radiation (λ=1.936Å). The examination with SEM took place in a 20 kV JEOL 840A SEM equipped with an EDAX analyzer (OXFORD ISIS 300) and the necessary software to perform linear microanalysis and chemical mapping of the examined substrate.

For the examination with TEM the floating dross samples, which were powder-like, were captured between silicon tiles, polished up to about 40 μm and afterwards thinned with ion bombardment. For the samples, which were bulk, only polishing and ion bombardment took place. The examination was accomplished in a 100 kV JEOL100CX TEM.

3. Results and discussion

3. 1. Characterization of the zinc ingot and the clean zinc bath

The first step of the present work was the characterization of the pure zinc ingots used in the

galvanizing process. Therefore one of them was cut in four pieces and about 50 particles in total were scratched from every surface of these pieces. These particles contain in average 99.89 wt.% Zn, as it was determined with EDS. No impurities were detected with this method because of its low sensitivity, although the chemical analysis of the product, which was provided by its producer, mentions also the presence of Pb, Cd, Fe, Cu and Sn at a total concentration of about 0.014 wt.%. In any case, impurities of this concentration, although they are dissolved in the molten Zn bath, they do not affect significally the structure of the coating [11-13].

Afterwards the clean Zn bath was examined. For this investigation about 15 samples (from each sampling depth as it was previously explained) were examined with EDS in order to determine their chemical composition. The average results are presented in Table 1, from which it is obvious that the concentration of the impurities is much higher than in the ingot.

Table 1. Results of the SEM microanalysis of the pure zinc bath.

Element	Concentration (wt.%)
Zn	98.70
Fe	0.5
Cl	0.4
Al	0.4

From these impurities Al is deliberately added to the zinc bath in order to improve the appearance of the final product [1], while Fe and Cl are transferred by the ferrous substate during its immersion in the liquid metal. Fe is also dissolved from the kettle walls. However, as it was mentioned earlier, impurities of so low concentration do not have any significant effect on the coating structure. Furthermore the Zn concentration in the bath remains high enough, so as to be close to the necessary concentration for the production of a good quality coating [11]. No nickel addition takes place at the industries that provided the samples, as it was stated by their chief engineers and consequently this metal was not detected. Other elements such as Sn, Cu and Cd that originate from the zinc ores were not detected because of the low sensitivity of EDS.

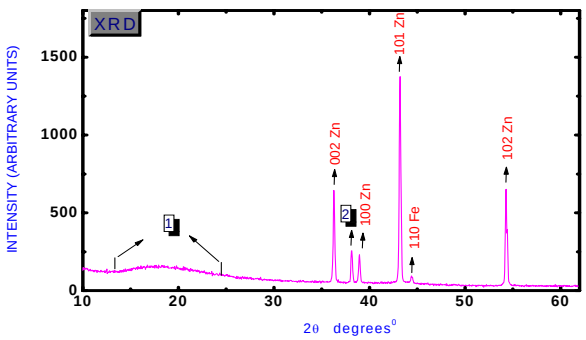

Fig. 2. XRD pattern of the pure zinc bath (1: amorphous Zn and Fe phases, 2: $ZnCl_2$).

The examination with XRD is in accordance with the EDS results. As a matter of fact, it verifies the presence of zinc, iron and amorphous zinc and iron chlorides (Fig. 2). TEM also detected pure Zn (PDF#040831 [14]), as it was expected. However, the diffraction patterns of Fig. 3a and 3b prove that, apart from pure Zn, Fe-Zn solid solutions and Fe-Zn phases (PDF#320478 and PDF#341314[14]) are present in the examined sample.

The presence of Fe-Zn solid solutions is indicated by the small shift of the zinc diffraction rings relatively to the position of the rings of pure Zn. These compounds are most probably formed during the solidification of the liquid sample, which was taken from the kettle, since the Zn bath contains a small concentration of dissolved Fe. They are not visible with XRD due to their low concentration.

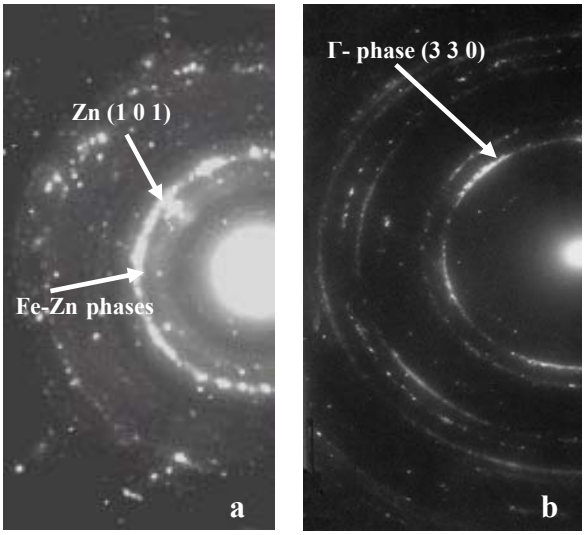

Fig. 3. Diffraction pattern of the zinc bath (a: Zn and Fe-Zn solid solutions, b: Γ-phase).

By contrast, the Fe-Zn phases is likely that they were already present in the liquid when it was collected from the kettle and not formed during its solidification, because these phases are insoluble in molten Zn and their melting point is higher than the temperature of the Zn bath [1]. This fact indicates that the cleaning of the zinc bath is incomplete since the perfect purification of a liquid metal in a large-scale industrial facility is very difficult. So, their presence is not peculiar. However, if we take in account that TEM is a very sensitive method and the fact that the XRD patterns do not include any peaks refering to these phases, it could be deduced that in this case their concentration is very low and consequently their effect is seemingly unimportant, at least when the Zn melt is clean.

3. 2. Characterization of the floating dross (galvanizing ashes)

The formation of the floating dross is accomplished in three steps. First a thin film is formed on top of the molten zinc. Afterwards, the thickness of this film gradually

increases, leading to a comparatively thick, compact layer with an average thickness of a few hundreds of microns. Finally this layer is partially oxidized from the kettle heat, while its volatile compounds are evaporated. Hence a powder similar to ash is formed. For the characterization of the floating dross, about 10 samples from each of these products were examined.

Table 2. Results of the SEM microanalysis of the floating dross samples.

Element	Concentration (wt.%)		
	1st Stage	2nd Stage	3rd Stage
C	0.3	0.2	-
O	28.0	42.1	58.2
Al	16.2	17.7	14.7
Cl	5.4	3.0	2.0
Zn	46.5	31.2	20.2
Pb	1.3	0.8	0.7
Fe	1.1	1.3	1.1
Ti	1.2	3.7	3.1

Three representative SEM micrographs of each stage are presented in Fig. 4a, b and c, while Table 2 averages the results of EDS microanalysis of each step. The formation of the thin film is obvious in Fig. 4a. At the surface of this film wrinkles are present, which were probably formed during the sampling procedure, as the liquid and the semi-molten sample suffered several deformations. Furthermore certain powder grains are present. Both these phases are probably metal oxides as Table 2 implies. By contrast, Fig. 4b clearly refers to a thicker film and Fig. 4c to a powder-like body composed by grains of different size.

The element, which is predominant in Table 2, is oxygen. Its concentration is high since the very beginning of the ash formation and it increases significantly at the next stages. This phenomenon implies that floating drosses are mainly composed by oxides. Every metal detected in dross could participate at the formation of these compounds. However, since the concentration of Zn and Al in the samples is much higher, it is possible to be deduced that the main oxides formed are ZnO and Al_2O_3.

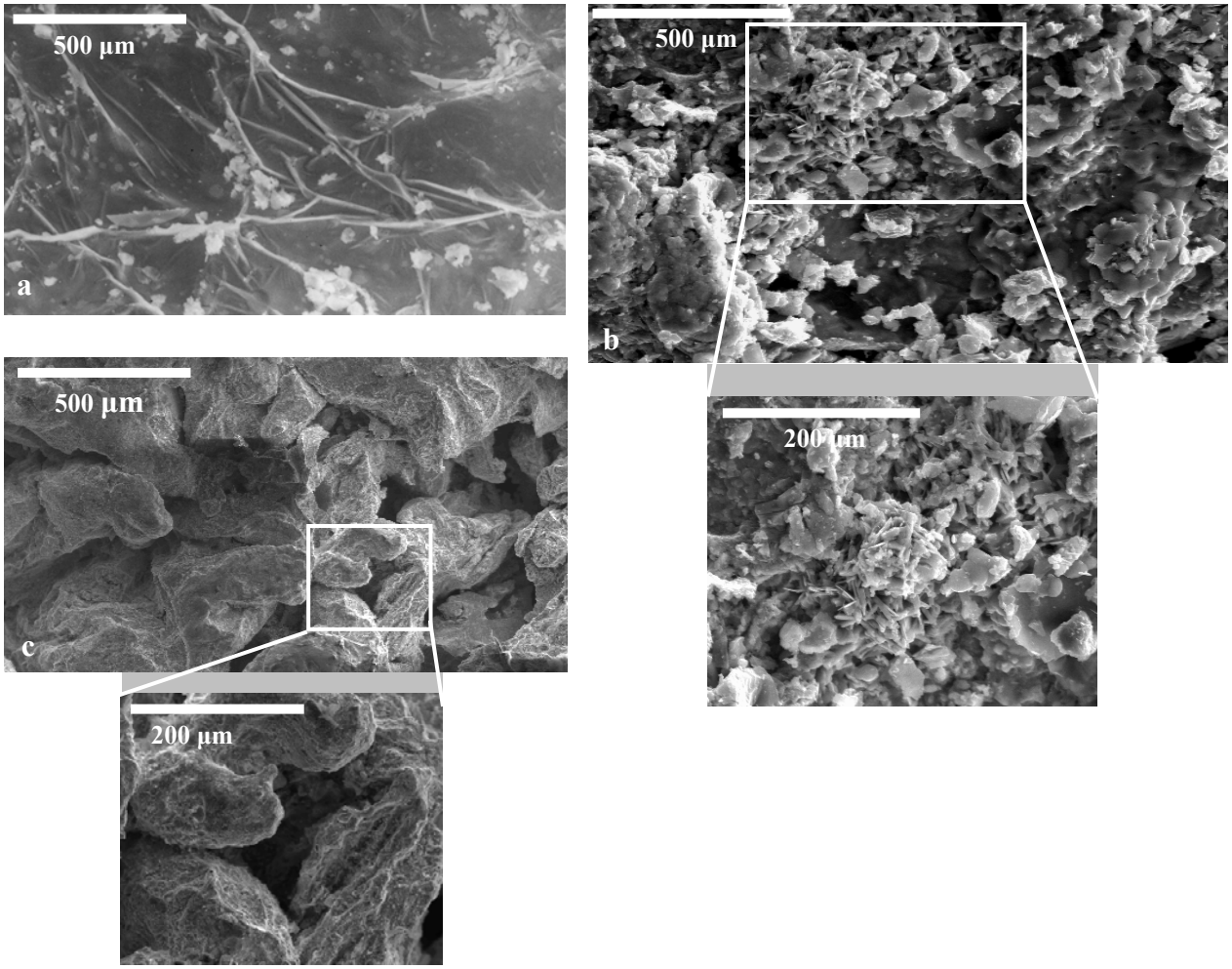

Fig. 4. SEM micrographs of the floating dross (a: first stage, b: second stage, c: third stage). The inset micrographs refer to the highlighted areas at higher magnification.

Furthermore, the formation of Fe-Al intermetallics at the first stage is rather limited, if it takes place at all, as the low Fe concentration implies. At the second stage the Fe concentration increases. Consequently at this stage the intermetallics formation is more probable.

What is unexpected in this table is the high Al concentration. As it was mentioned in Table 1, the average Al concentration in the zinc bath is about 0.3%. This is also the Al concentration that litterature suggests for batch hot-dip galvanizing [1]. However, Table 2 shows that Al concentration is more than 14 wt.%. This phenomenon could be explained by the fact that Al is much lighter than Zn (d_{Zn}=7.140 g/cm^3 at 20^{o}C, d_{Al}=2.70 g/cm^3 at 20^{o}C [15]). Therefore it floats on top of the Zn melt. This means that the dissolved Al is not uniformly distributed in the bath, but most of it is gathered close to the top.

Another peculiar phenomenon concerning the ashes composition is the high Ti concentration. Ti is also much lighter than Zn (d_{Ti}=4.50 g/cm^3 at 17.5^{o}C [16]) and it is possible to float on the Zn melt. However, while Ti could improve the coating quality [15, 17], it is not used in the industries that provided the samples, as the chief engineers of these facilities declared. Furthermore its concentration in the Zn ingots is almost nul. Concequently, its presence could be explained only by taking into account the fact that the molten zinc is covered with vermiculite. This compound offers thermal insulation to the upper surface of the liquid metal and consequently diminishes its thermal losses resulting to important energy savings. This material is mainly composed by hydrated magnesium-iron-aluminum silicate [18]. However, it also contains Ti at a concentration about 1-3 wt.% [18], part of which is probably dissolved in the liquid zinc.

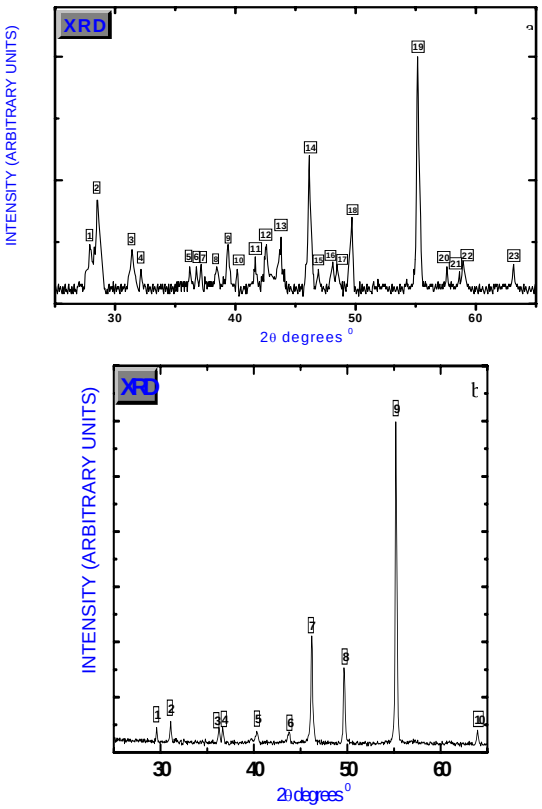

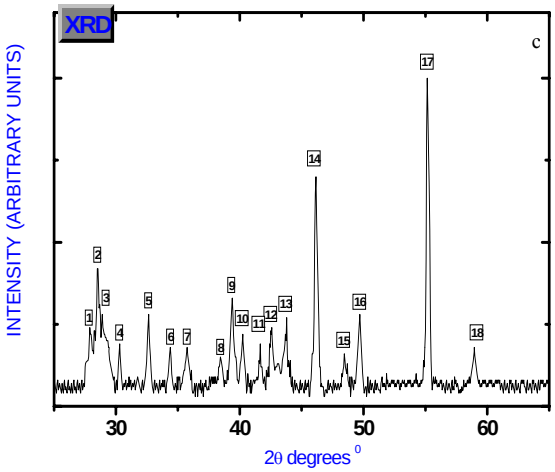

Fig. 5. XRD patterns of the floating dross (a: first stage, b: second stage, c: third stage). The peaks are summarized in Table 3.

Table 3. Compounds detected with X-ray diffraction in the floating dross.*

Compounds	Peaks of Fig. 5a	Peaks of Fig. 5b	Peaks of Fig. 5c
Al_2O_3	9, 11, 14, 15, 16, 17, 18	2	7, 9, 11, 14, 15, 16
ZnO	3, 5, 6, 10, 13, 23	3, 5, 6	6, 7, 10, 13
Mixed Al-Zn-Fe oxides	8, 12	1	4, 5, 8, 12
$ZnCl_2$	4, 7, 21, 22	-	-
Fe-Zn-Al intermetallics	19	8	17
Zn-Al-Ti intermetallics	1, 2, 21	4	1, 2, 3, 6, 18
Al	20	-	-
Zn	-	7, 8, 10	-

*The identification of the phases was performed using the Powder Diffraction Files. For each compound one or more PDF cards were selected (e.g., ZnO: PDF #800075, PDF#890511[14]).

The above assumptions were verified with XRD and TEM. The XRD patterns are presented in Fig. 5a, 5b and 5c. Concerning the pattern of Fig. 5a, most of the peaks recorded refer to Zn and Al oxides, as Table 3 shows. Nevertheless, a few peaks refer to Fe-Zn-Al intermetallics, pure Al, pure Zn and Zn-Al-Ti intermetallics. A volatile compound ($ZnCl_2$) was also detected, which is not present in the patterns of the latter stages, probably due to sublimation. This compound is used at the final stage of

the pretreatment of the ferrous substrates (fluxing). During this stage the substrate is immersed in a bath of an aqueous solution containing about 50 wt.% of $ZnCl_2 \cdot 2NH_4Cl$. This salt covers the steel surface in order to protect it from further oxidation prior to hot-dipping [1] and most of it is sublimated when steel comes in contact with the molten zinc. However a small quantity is possible to remain on top of the molten zinc, especially as far as it concerns $ZnCl_2$, because this compound is less volatile than NH_4Cl, as it is possible to be deduced by comparing the vapor pressure of $ZnCl_2$ (1 mmHg at 428°C [16]) and the vapor pressure of NH_4Cl (1 mmHg at 160,4°C [16]). By comparing the patterns of Fig. 5a, 5b and 5c, it is also obvious that during the second stage the pure metals are absent because of their oxidation.

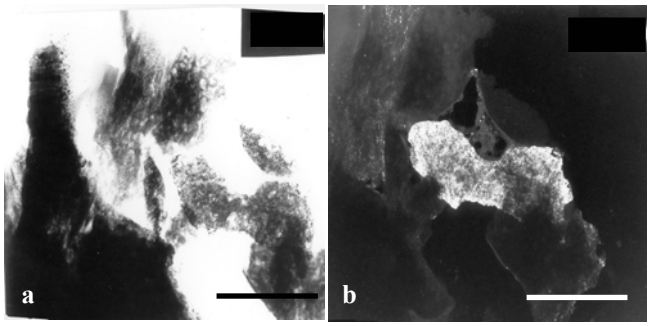

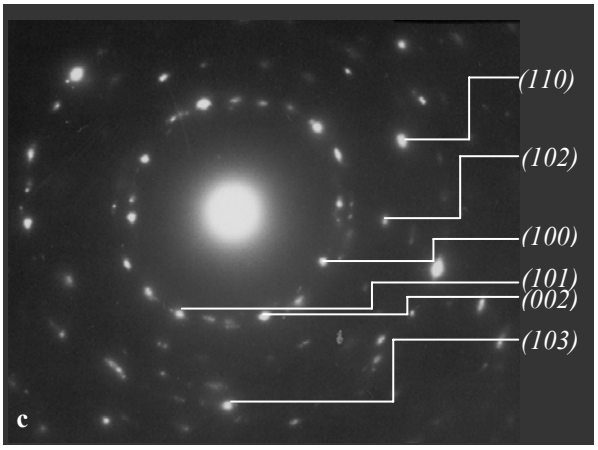

Fig. 6. (a) Bright field TEM micrograph of a ZnO particle (Bar = 0.1 μm), (b) Dark field TEM micrograph of the area of Fig. 6a (Bar = 0.1 μm), (c) Electron Diffraction pattern of Fig. 6b referring to ZnO (PDF #361451[14]).

The examination with TEM verified the presence of ZnO (PDF#361451[14]-Fig. 6 and 7), Al_2O_3 (PDF # 832081 [14] -Fig. 8) and several mixed oxides such as $Zn(Al_{1.9}Fe_{0.1})O_4$ and $Zn(Al_{1.4}Fe_{0.6})O_4$ (PDF#821044 [14]-Fig. 9a and PDF#821046 [14]-Fig. 9b). Having the accurate value of the camera constant, the indexing of the diffraction pattern of Fig. 9b was accomplished as it is presented in Table 4.

Table 4. Experimental and calculated d-values for the indexed rings of the electron diffraction pattern of Fig. 9b.

hkl	d_{exp}	d_{cal}
220	2.85	2.897
311	2.48	2.471
400	2.03	2.049
331	1.84	1.880
422	1.66	1.673
511	1.56	1.577
442	1.35	1.366

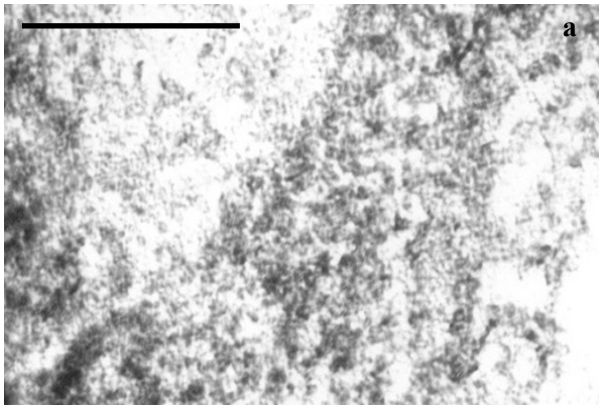

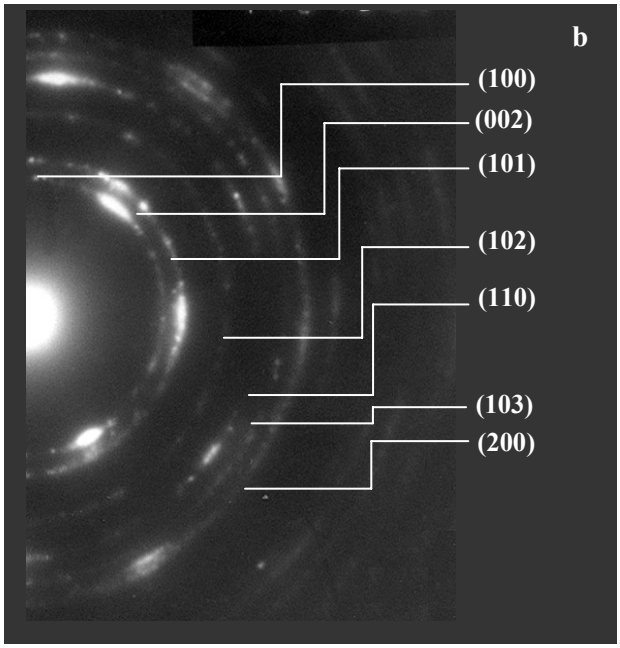

Fig. 7. (a) Bright field TEM micrograph of a ZnO particle (Bar = 0.1 μm), (b) Electron Diffraction pattern of Fig. 7a referring to ZnO (PDF #361451[14]).

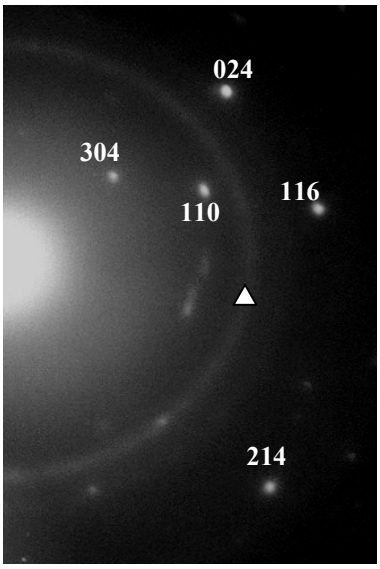

Fig. 8. Diffraction pattern of Al_2O_3. The ring, which is pointed out with "Δ", refers to Zn.

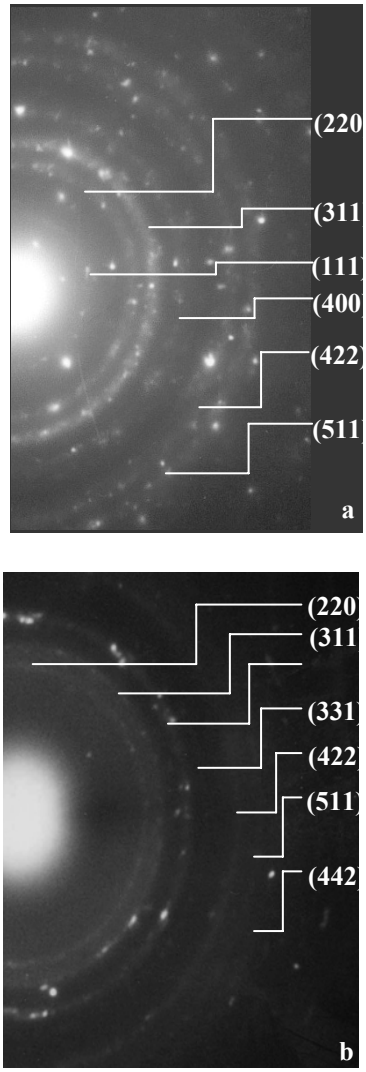

Fig. 9. Electron diffraction pattern of $Zn(Al_{1.9}Fe_{0.1})O_4$ (a) and $Zn(Al_{1.4}Fe_{0.6})O_4$ (b) taken from dross sample.

3. 3. Characterization of the bottom dross

As it was mentioned before, the bottom dross is usually removed from the Zn kettle by mechanical means (special shovels). This method results to the simultaneous removal of an important Zn quantity during the cleaning of this byproduct. This phenomenon is obvious at the SEM micrographs, which were recorded (Fig. 10a and 10b). Three phases are observed in these micrographs. One of them is lighter and appears like "islands" inside the second phase, which looks like a darker "sea". Many white spots are also scattered in the second phase. Also, in both micrographs a few dark spots are present, which refer to voids, probably formed because of the slow solidification process of the liquid metal after its removal from the zinc kettle. Furthermore, in both micrographs there are straight lines formed because of the imperfect polishing of the specimens prior to the observation with SEM.

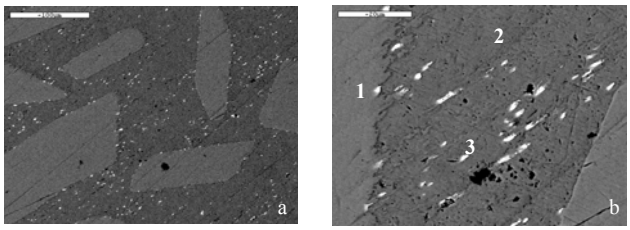

Fig. 10. SEM micrograph of the bottom dross (a: x450, b: x2000, focus on the darker area between the lighter fragments).

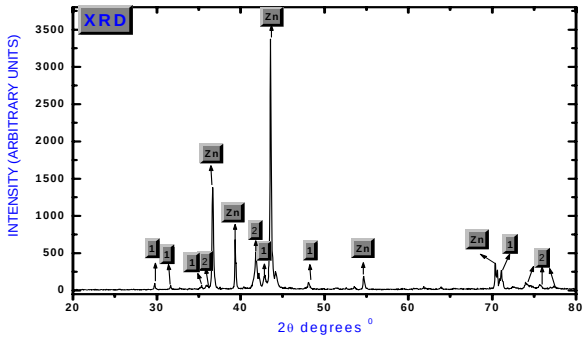

Fig. 11. XRD pattern of the bottom dross. Peaks noted with #1 and #2 refer to the ζ-phase of the Fe-Zn phase diagram.

Table 5. Results of the SEM microanalysis of the bottom dross samples. The numbers of the phases refer to Fig. 10b.

Phase Number	Concentration (wt. %)	
	Zn	Fe
1	99.7	0.3
2	93.8	6.2
3	53.2	46.8

The results of the microanalysis of the above-mentioned phases are summarized in Table 5, where the average of the data recorded from 20 points from each one

of these phases is presented. This table shows that the darker area between the lighter fragments (phase #1 in Fig. 10b) is composed almost exclusively by Zn. This is probably the liquid Zn trapped in the device used for the cleaning of the kettle. The white spots (phase #3 in Fig. 10b) observed in this phase contain a large amount of Pb. Pb is added in the molten Zn in order to diminish the surface tension of the liquid and consequently reduce the coating thickness [13]. However the Pb solubility in liquid Zn is low, therefore a layer of molten Pb precipitates at the bottom of the Zn kettle. It is likely that this layer is the source of Pb in the examined specimen. The lighter areas of the dross (phase #2 in Fig. 10b) are mainly composed by Zn, while they contain also about 6 wt.% Fe. This composition is typical for the ζ (zeta) phase of the Fe-Zn phase diagram [1]. This phase is isoluble in molten Zn and its melting point (about 530°C [1]) is higher than the kettle temperature (about 450°C). Consequently, particles of this phase, formed when the Fe concentration in the kettle is above its solubility, precipitate at the bottom of the liquid Zn. This could be considered as the main byproduct, while Zn and Pb are removed because of the imperfect method used for the cleaning process. The presence of Zn and the ζ-phase was also identified with XRD (Fig. 11).

3. 4. Characterization of the blowing waste

As it was mentioned before, the blowing waste is a byproduct formed only in tube galvanizing after hot-dipping. By contrast to the bottom dross whose the specimens are bulk, the blowing waste is powder-like. Therefore it is mainly composed by spheres as it is possible to be seen at the SEM micrographs of Fig. 12.

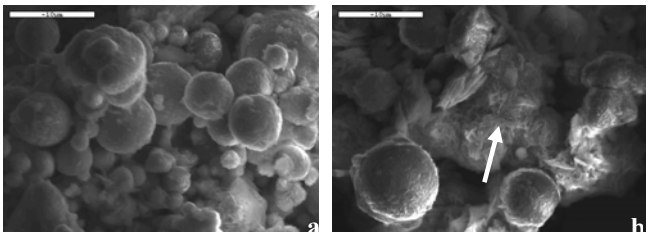

Fig. 12. SEM micrographs of two different grains of the blowing waste. In Fig. 12b the arrow points the needle-like crystals that are observed.

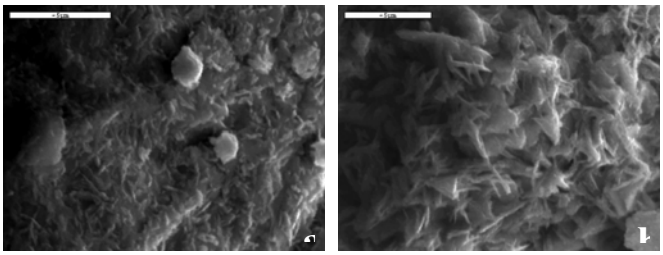

Fig. 13. SEM micrographs of the needle-like phase formed on the grains of the blowing waste.

These spheres are formed through the solidification of Zn droplets during blowing. As their microanalysis shows (Table 6) only Zn and O are present in them. Consequently, they are probably composed by a core of pure Zn covered with a layer of ZnO. The data of Table 6 is the average of the microanalysis 20 different spheres.

However some needle-like crystals are also observed at the micrographs of Fig. 12. These crystals could be better observed in Fig. 13, where a similar area is observed under higher magnification (x9000). Their microanalysis (Table 6) indicates that these crystals are mainly composed also by Zn and O with a mole proportion equal to 1:1. Hence, these crystals are probably pure ZnO. The presence of Zn and ZnO is also verified with XRD and Table 7 (Fig. 14, ZnO-PDF#211486 [14], Zn-PDF#040831 [14]).

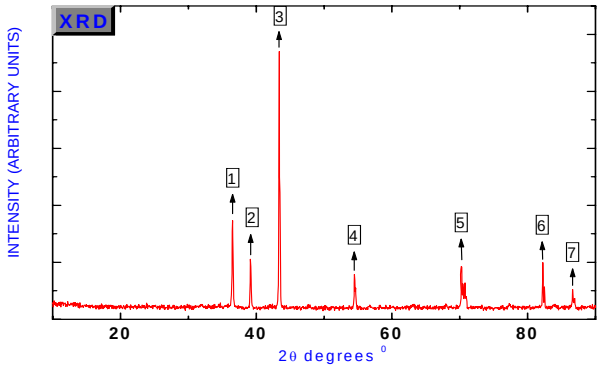

Fig. 14. XRD pattern of the blowing waste.

Table 6. Results of the SEM microanalysis of the blowing waste samples.

Phase	Concentration wt.%	
	Zn	O
Spheres	91.3	8.7
Needles	20.3	79.7

Table 7. Compounds detected with X-ray diffraction in the blowing waste [14].

Compounds	Peaks of Fig. 14
Zn	1, 2, 3, 4, 5, 6, 7
ZnO	1, 4, 6

4. Conclusions

From the above investigation it was deduced that galvanizing byproducts contain large amounts of zinc in different forms. In particular floating dross (galvanizing ashes), which is formed at three stages, after the final stage is mainly composed by different oxides (mainly ZnO and Al_2O_3), while other compounds (such as Zn-Al-Fe intermetallics) are also present. By contrast, in bottom dross mainly crystallites of the ζ-phase of the Fe-Zn phase diagram scattered in a matrix of pure Zn were detected. Finally, blowing waste, which is in powder form, is

composed by spheres whose the core is of pure Zn covered with a layer of ZnO. Hence these compounds could be used as row materials for zinc recovery or for other processes for the production of different zinc compounds although the large Fe concentration could be a certain drawback.

References

[1] A. R. Marder, Prog. in Mat. Sci. **45,** 191 (2000).
[2] F. Cinar Sahin, B. Derin, O. Yucel, Scan. J. of Met. **29**, 224 (2000).
[3] G. Reumont, R.S. De Figueiredo, J. Foct, J. Mat. Sci. Let. **18**, 1879 (1999).
[4] G. P. Lewis, J. Pedersen, 3rd Asian Pacific Galvanizing Conference, Melbourne, Australia, 1996, p. 1.
[5] Galvanizing Reactive Steels-A guide for Galvanizers and Specifiers, International Lead Zinc Research Association, N. Carolina (1996).
[6] D. Horstmann, Faults in Hot Dip Galvanizing, Stahleisen M.b.H., Dusseldorf (1975).
[7] M. K. Jha, V. Kumar, R. J. Singh, Res. Cons. and Rec. **33**, 1 (2001).
[8] M. A. Rabah, A. S. El-Sayed, Hydromet. **37**, 23 (1995).
[9] G. Vourlias, N. Pistofidis, G. Stergioudis, E. K. Polychroniadis, Sol. St. Sci. **7**, 465 (2005).
[10] G. Vourlias, N. Pistofidis, El. Pavlidou, G. Stergioudis, E. K. Polychroniadis, accepted for presentation in Romanian Conference of Applied Physics, Bucharest (2006).
[11] ASTM B6, Standart Specification for Zinc.
[12] N. Katiforis, G. Papadimitriou, Surf. Coat. Tech. **78**, 185 (1996).
[13] G. Vourlias, N. Pistofidis, G. Stergioudis, Crys. Res. Tech. **39**, 23 (2004).
[14] PC Powder Diffraction Files, JCPDS-ICDD, 2000.
[15] G. Reumont, T.Gloriant, P.Perrot, J. Mat. Sci. Lett. **15**, 445 (1996).
[16] R. H. Perry, C.H. Chilton (editors), Chemical Engineers' Handbook, 5th ed., McGraw-Hill, New York (1977).
[17] G. Reumont, T. Gloriant, P. Perrot, J. Mat. Sci. Lett. **14**, 752 (1995).
[18] Informative Booklet on Vermiculite, The Vermiculite Association, UK (2003).

*Corresponding author: polychr@auth.gr